J Polym Res (2010) 17:221–232
DOI 10.1007/s10965-009-9308-5

ORIGINAL PAPER

# Physical properties and biodegradation of acrylic acid grafted poly(ε-caprolactone)/chitosan blends

**Yeh Wang · Jiang-F. Yang**

Received: 22 December 2008 / Accepted: 6 May 2009 / Published online: 23 May 2009


**Abstract** We blended films of acrylic acid grafted polycaprolactone (PCLgAA) and citosan (CS) with different compositions from aqueous acetic acid solution. DSC measurements showed that the melting temperatures and enthalpies of the blends decreased with increasing CS content. From FTIR results, we observe that the amino groups of CS form covalent bonds with the carboxylic groups of PCLgAA in addition to hydrogen bonds between the constituents in the blends. Though the crystal structure of the PCLgAA component was not changed, as proved by WAXD results, blending CS suppressed the crystallinity of the blends. Furthermore, the ductility of CS was increased during tensile testing in PCLgAA/CS blends due to enhanced affinity between the two components. However, PCLgAA/CS blends show greater resistance than PCL/CS blends to biodegradation in an enzymatic environment.

**Keywords** Polycaprolactone · Chitosan · Polymer blend · Biodegradable polymer · Enzymatic degradation

## Introduction

Chitosan (CS) is a natural polymer, derived by N-deacetylation of chitin, the second most abundant biopolymer in nature after cellulose [1]. In general, chitin is present in crustaceans such as shrimps, crabs and lobsters, as well as certain fungal cell walls. Chitosan has received growing attention, since it is biodegradable, biocompatible and relatively inexpensive. Besides its availability from renewable resources, chitosan offers unique physical, chemical, and biological properties, which have been studied for various applications [2]. In recent decades, the application of CS has reached vascular surgery, tissue culture, and tissue regeneration as a hemostatic agent [3]. However, CS has a high modulus of elasticity, owing to the high glass transition temperature and crystallinity [4]. The film brittleness and great sensitivity to moisture of CS limit its broader application as a biomaterial.

In order to overcome these issues, various methods are applied to associate CS with hydrophobic polymers to improve its morphology and ductility. Many CS copolymers have been chemically synthesized. Since the molecular chains of CS hold functional groups, novel polysaccharide derivatives containing poly(ethylene glycol) (PEG) [5], poly(vinyl alcohol)(PVA) [6], and poly(methyl methacrylate) (PMMA) [7] have been synthesized by copolymerization. Depending on chemical structure and composition, the properties of these copolymers vary widely. When CS is grafted with PEG, the modulus of elasticity and the elongation at break are improved by the suppression of crystallinity of each component [5]. Moreover, the drug release behavior of copolymers based on CS can be adjusted by changing the kinds of grafted polymers and their graft degree [8]. The other method is to prepare blends consisting of CS and other polymers, for example PVA [9], poly(ethylene oxide) (PEO) [10,11] and polylactide [12]. Taking advantage of amino and hydroxyl groups on the molecular chains, CS is very useful in the development of composite materials such as blends or alloys with other materials. The blending of CS with other polymers not only changes its morphology but also improves its toughness. Compared with chemical copolymerization, blending is still a relatively simple, cost effective, and convenient way to improve the properties of CS.

Y. Wang (✉) · J.-F. Yang
Department of Chemical Engineering, Tunghai University, Taichung, Taiwan 407, Republic of China
e-mail: yehwang@thu.edu.tw

Currently, there is considerable interest in the blending of CS with biodegradable polyesters because it is an effective approach to reduce environmental pollution from plastic wastes. Among many linear polyesters, poly(ε-caprolactone) (PCL) has attracted the most attention. PCL is one of the commercially available non-toxic biodegradable thermoplastics. It has suitable mechanical properties with a low glass transition, which translates into rubber-like toughness. Furthermore, PCL is a polymer which demonstrates biocompatibility and the capacity for drug transport. It is relatively hydrophobic and has a slow degradation rate, ideal for use as bone substitutes and sustained release drug carriers. However, on its own, PCL cannot be prepared for bone substitute due to its low modulus, typically 350–450 MPa.

Inoue's group [13–15] reported blending films of PCL/chitin and PCL/CS by solution-casting technique using 1,1,1,3,3,3-hexa-fluoro-2-propanol (HFIP) as the common solvent, then investigated their thermal properties and crystallization behavior. The results showed that chitin and CS components suppressed the crystallization of PCL component, resulting in decreasing crystallinity of PCL. In fact, there are few common solvents for CS and linear polyesters except HFIP, which is very expensive and difficult to dry. Olabarrieta et al. [16] studied the transport properties of PCL/CS blend with the co-solvent of acetic acid and chloroform, which showed reduction of water vapor permeability. The SEM micrograph of the composite membrane indicated phase separation of the two components. Sarasam and Madihally [17] prepared the PCL/CS blends by solution-casting in a common solvent of aqueous acetic acid. They reported that the 50 wt% oven-dried blend membrane showed significant improvement in mechanical properties as well as support for cellular activity relative to CS. In all cases, the choice of common solvent is closely related to morphology properties of the blends.

Adhesion of the two polymers can be facilitated by using a compatibilizer to improve the compatibility between the two immiscible phases, thereby improving the mechanical properties of the composite [18]. Avella et al. [19] showed that by using pyromellitic anhydride as a compatibilizer, modification of PCL on its terminal groups increased its compatibility with plasticized starch. Wu [20] used acrylic acid grafted PCL to prepare the PCLgAA and CS composites by melt blending with CS as the minor component. The PCLgAA properties were improved more than that of PCL due to the enhanced compatibility with CS. This suggests that grafting a reactive functional group onto PCL in a PCL/CS blend is likely to produce a blend that offers the best combination of low cost and practical mechanical properties. However, the melt-blended composites would not be suitable for medical use with the phase-separated morphology, where the coarse CS particles were dispersed in the PCL matrix.

In this study, the effect of grafting acrylic acid onto PCL in the PCLgAA/CS blends on the structure and thermal properties of the solution-casting membranes was investigated. The composite films of various compositions were characterized using differential scanning calorimetry (DSC), FTIR spectroscopy, WAXD, and scanning electron microscope to identify the structural changes caused by the grafting of acrylic acid. Tensile properties were measured with a universal tensile tester. Additionally, weight loss of blends exposed to an enzymatic environment was determined in order to assess the biodegradability of the blend membranes.

## Materials and methods

PCL with molar mass of 57 kD by SEC (size exclusion chromatography) measurement from Solvay was used as received. Acrylic acid (AA) of regent grade was supplied by Acros. PCLgAA was synthesized from these constituents in our laboratory. Benzoyl peroxide (BPO by Acros), initiator in the grafting reaction, was purified by dissolving in chloroform and reprecipitating with methanol. Chitosan with molar mass of 422 kD (SEC measurement) and degree of deacetylation (DD) at 86% (colloidal titration) was supplied by Qingdao Golden Garden Biological Products Co., China. For the enzymatic exposure test, lysozyme of hen egg white was purchased from Bionovas, USA. It was reported by the manufacturer to have a specific activity of 50000 U/mg. All other chemicals used were of reagent grade.

### Grafting reaction of PCLgAA

A mixture of AA and BPO was added with PCL pellets to allow grafting to take place in an internal mixer, a Brabender PL 2000 plasticorder. . The BPO loading and AA loading were maintained at 0.3 and 10 wt%, respectively. The reactions were carried out at 85 °C. Preliminary experiments of torque and temperature measurements showed that reaction equilibrium was attained in 6 h, and reactions were, therefore, allowed to progress for 6 h, at a rotor speed of 60 rpm. About 2 g of grafted PCL was heated for 2 h in 200 ml of refluxing xylene. This solution was then titrated immediately with a 0.03 N ethanolic KOH solution, which had been standardized against a solution of potassium hydrogen phthalate, with phenolphthalein used as an indicator. The degree of grafting were calculated using the following equations [21]:

$$\text{Degree of grafting}\% = \frac{C_{KOH}(N) \times V_{KOH}(ml) \times 72}{polymer(g)} \times 100\% \quad (1)$$

With BPO loading and AA loading at 0.3 and 10 wt%, respectively, the degree of grafting was then determined at 8.75 wt%. Moreover, the molar mass of PCLgAA was 55 kD measured by SEC, indicating that the base PCL was slightly degraded during grafting reaction.

### Formation of solutions and blends

Chitosan was dissolved in 0.5 M acetic acid and PCL or PCLgAA in glacial acetic acid in a laminar flow hood. Three milliliters of 1% chitosan solutions were slowly added to 10 mL of 0.1%, 0.3% and 0.9% PCL and PCLgAA solutions to obtain blends of 25%, 50% and 75% PCL and PCLgAA, respectively. The mixtures were stirred at room temperature for 2 min to obtain homogeneous solutions. In all the blends, the solvent composition was kept constant. Blend membranes were prepared by pouring homogeneous solutions into teflon coated dishes and oven dried overnight at 55 °C, and then vacuum dried at 55 °C for two days when no weight change was detected.

### Differential scanning calorimetry

Thermal properties of various blend membranes were characterized using a Perkin-Elmer DSC Pyris 1 (Perkin Elmer, Boston, MA). Nitrogen at the rate of 20 mL/min was used as purge gas. Five to ten mg of samples were sealed in aluminum pans and heated up to 100 °C and maintained at that temperature for about 5 min in order to erase the thermal history of the samples. They were cooled to 25 °C from where they were ramped from room temperature to 100 °C at a heating rate of 10 °C/min. The melting temperature of PCL was taken as the temperature at which the endothermic peak occurred during the second heating run.

### FTIR measurement

The samples used for FTIR measurements were cut to be thin enough to ensure that the observed absorption was within the linearity range of the detector. The FTIR spectra were recorded on an IR Prestige-21 instrument (Shimadzu Co, Ltd, Tokyo) by the transmission method at room temperature in the range from 3500–1000 $cm^{-1}$ at a resolution of 4 $cm^{-1}$ and with an accumulation of 16 scans.

### Wide-angle X-ray diffraction

Wide-angle X-ray diffraction (WAXD) patterns of blend samples were recorded on a Schimadzu XRD-6000 (40 kV/40 mA). The nickel-filtered Cu K$\alpha$ X-ray beam with a pinhole graphite monochromator ($\lambda$=0.15418 nm) was used as the source. WAXD patterns were measured in a $2\theta$ range of 5°–35° at a scanning rate of 1◦ min–1 at equal increment of 0.02°.

### Tensile testing of membranes

Rectangular strips of 40×7.5 mm size were cut from each membrane and strained to break at a constant crosshead speed of 10 mm/min using INSTRON 5842 (INSTRON Inc., Canton, MA). The thickness of the membranes was measured with a thickness gauge. Using the associated software Merlin (INSTRON Inc), break stress and strain were determined. The elastic modulus was calculated from the slope of the linear portion of the stress–strain curve. Samples were tested in dry state.

### Field emission scanning electron microscopy

The morphologies of the surfaces of the films, before and after enzymatic degradation, were observed with a field-emission scanning electron microscope (FESEM) JSM-5200 (JEOL, Japan), after being metallized using an ion coater IB-3 (Giko, Japan).

### Enzymatic degradation

Each film with dimension of 10×10×0.05 mm was put into a flask, which was filled with 100 ml phosphate buffer silane (PBS, PH 7.4) that contained 100 mg/L lysozyme. The flask was kept in a shaking bath at 37 . After incubation for a predetermined time, the films were washed well with deionized water, dehydrated using absolute alcohol, and dried to constant weight in a vacuum desiccator at ambient before analysis. The weight losses of the films were calculated and averaged over three specimens.

## Results and discussion

### Differential scanning calorimetry

Because the temperature in the heating range during DSC scans is lower than the $T_g$ of CS estimated at 203 °C [22], DSC has not detected any melting temperatures of CS, and only the thermal properties of PCL and PCLgAA are available. Figure 1a, b show the DSC curves of both PCL and PCLgAA, and their blends with CS with different compositions in the heating run. Both PCL and PCLgAA are observed as a crystalline polymer with single melting temperatures of about 67 °C and 63 °C, respectively (as seen in Table 1). No obvious glass transition is observed in the DSC heating curve, presumably owing to their low Tg ( ca. –60 °C) that are lower than the DSC low temperature limit.

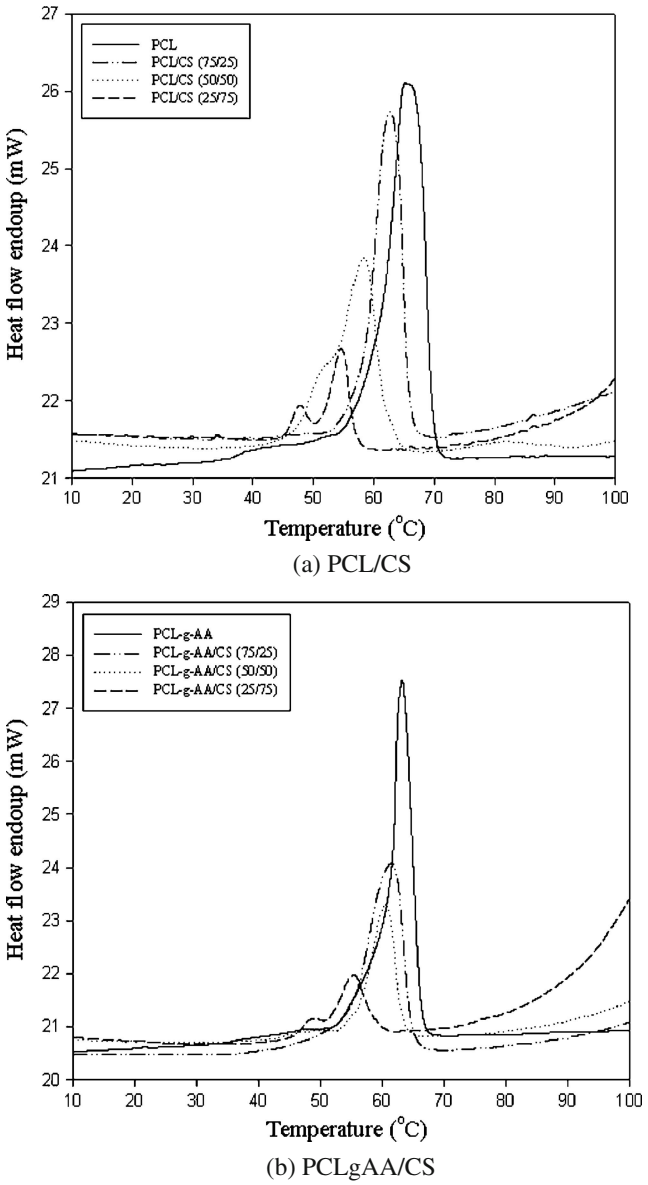


**Fig. 1** DSC curves of PCL, PCLgAA and their CS blends with different compositions. (**a**) PCL and PCL/CS blends; (**b**) PCLgAA and PCLgAA/CS blends

Both the PCL and PCLgAA/CS blends with the composition up to 50 wt% of CS clearly showed a single melting peak during heating. As the CS content further increased, the melting peaks of the blends gradually shift to lower temperatures, and their intensities obviously became weaker. Table 1 lists the DSC data of PCL and PCLgAA, and their CS blends with different compositions during heating. For PCL/CS blends, when CS content increased from 25% to 50%, the Tms of the blend decrease from 62.7 to 58.6°C, and the melting enthalpy also declined from 47 to 28 J/g. However, at 50 wt% of CS, a broad hump preceded the melting peak at 58.6°C. As the CS content reached 75 wt%, a double melting transition was displayed with peak temperatures at 49.0 and 54.7°C, respectively (Fig. 1a)., This indicated that blending PCL with CS affected its crystallization due to specific interaction between PCL and CS, which will also be investigated by FTIR spectrum later. Overall PCLgAA/CS blends behaved similarly (Fig. 1b) with their $T_m$s and melting enthalpies decreasing with increasing CS content. However, there seemed no broad hump in the DSC curve at 50 wt% of PCLgAA/CS blend. And the double melting peaks at 49.5 and 55.4°C also appeared at 75 wt% of CS. They were even broader than that of the PCL blend, indicating strong interaction between PCLgAA and CS due to the grafted carboxylic groups.

The melting enthalpy of the polymer is closely related to its crystallinity. Taking the component effect into account, the crystallinity (Xc) of PCL phase can be calculated using the following relation.

$$Xc_{,PCL} = \Delta H_m/(w \times \Delta H_o) \quad (2)$$

where $\Delta H_o$ is the thermodynamic enthalpy of fusion per gram of a fully crystalline PCL. Its value is taken as 142 J/g [23]; $\Delta H_m$ is the apparent enthalpy of fusion per gram of the blends; and w is the weight fraction of PCL in the blend.

The values of the melting temperature ($T_m$), melting enthalpy ($\Delta H_m$) and the degree of crystallinity ($Xc_{,PCL}$) of all samples were listed in Table 1. With increasing CS content in the blend film, the values of $\Delta H_m$ and $Xc_{,PCL}$ became smaller, and $T_m$ shifted to lower temperatures. The changes in $T_m$, $\Delta H_m$ and $Xc_{,PCL}$ were due to the formation of intermolecular hydrogen bonds between the carbonyl groups of PCL or PCLgAA and hydrogen-donating groups of chitosan, ie hydroxyl, amide and amine groups, as proposed in a previous report [13]. The formation of intermolecular hydrogen bonds should occur in the amor-

**Table 1** DSC data and crystallinity of PCL, PCLgAA and their CS blends

| Sample composition | Melting temp. $T_m$( ) | | Heat of fusion $^{\triangle}H_m$(J/g) | | Xc(%) | |
|---|---|---|---|---|---|---|
| | PCL | PCL-g-AA | PCL | PCL-g-AA | PCL | PCL-g-AA |
| 100/0 | 65.3 | 63.3 | 63.1 | 61.3 | 44.4 | 43.2 |
| 75/25 | 62.7 | 61.6 | 46.8 | 45.7 | 44.0 | 42.9 |
| 50/50 | 58.6 | 60.6 | 28.3 | 26.6 | 39.9 | 37.4 |
| 25/75 | 54.7 | 55.4 | 12.4 | 9.0 | 34.9 | 25.4 |

phous phase, so that the crystallization of polymers waas suppressed. The main reason for the decrease in $T_m$ was that CS was distributed on a very fine scale, and interfered with the growth of crystalline lamella. Note that the PCLgAA blends showed a lower $Xc_{,PCL}$ than corresponding PCL blends. CS is a rigid polymer with strong intramolecular hydrogen bonds on the backbone. When CS was blended with PCL or PCLgAA, molecular chains of the polyester components were trapped in the glassy environment because the heating range is lower than $T_g$ of CS. The mobility of polymer segments was hindered by CS rigid molecular chains, and the perfection of the crystals became worse. Thus $T_m$s of the PCLgAA blends decreased faster with CS content than that of the PCL blends due to stronger intermolecular interactions between PCLgAA and CS.

## FTIR analysis

FTIR spectroscopy is especially valuable in analyzing the phase structure and the miscibility in the blends of PCL and PCLgAA with CS. The IR spectrum of both PCL and PCLgAA (see Fig. 2a, b) showed a prominent characteristic absorption centered about 1725 $cm^{-1}$, attributable to carbonyl stretching absorption. There exists an obvious extra peak at 1710 $cm^{-1}$ for the grafted PCL. This extra peak is characteristic of –C=O representing the free acid in the modified polymer. This peak at 1710 $cm^{-1}$, as well as a broad –OH stretching absorbance at 3000–3400 $cm^{-1}$, also reported elsewhere [24,25], demonstrated that AA had been grafted onto PCL. In addition, the FTIR spectra in these figures also showed the overlapped bands in the region of 3200–3700 $cm^{-1}$, which are assigned to the –NH and –OH stretching bands of CS [26], and became weaker with decreasing CS content. These bands, which were mainly caused by the –NH group of CS [27] representing overlapped intramolecular and intermolecular hydrogen bonds, were much more intense than the –OH stretching absorbance observed in the absence of CS. Next in the blends of PCL/CS (Fig. 2a), the peak intensities of the two bands associated with amide linkage in CS, 1644 $cm^{-1}$ (symmetric

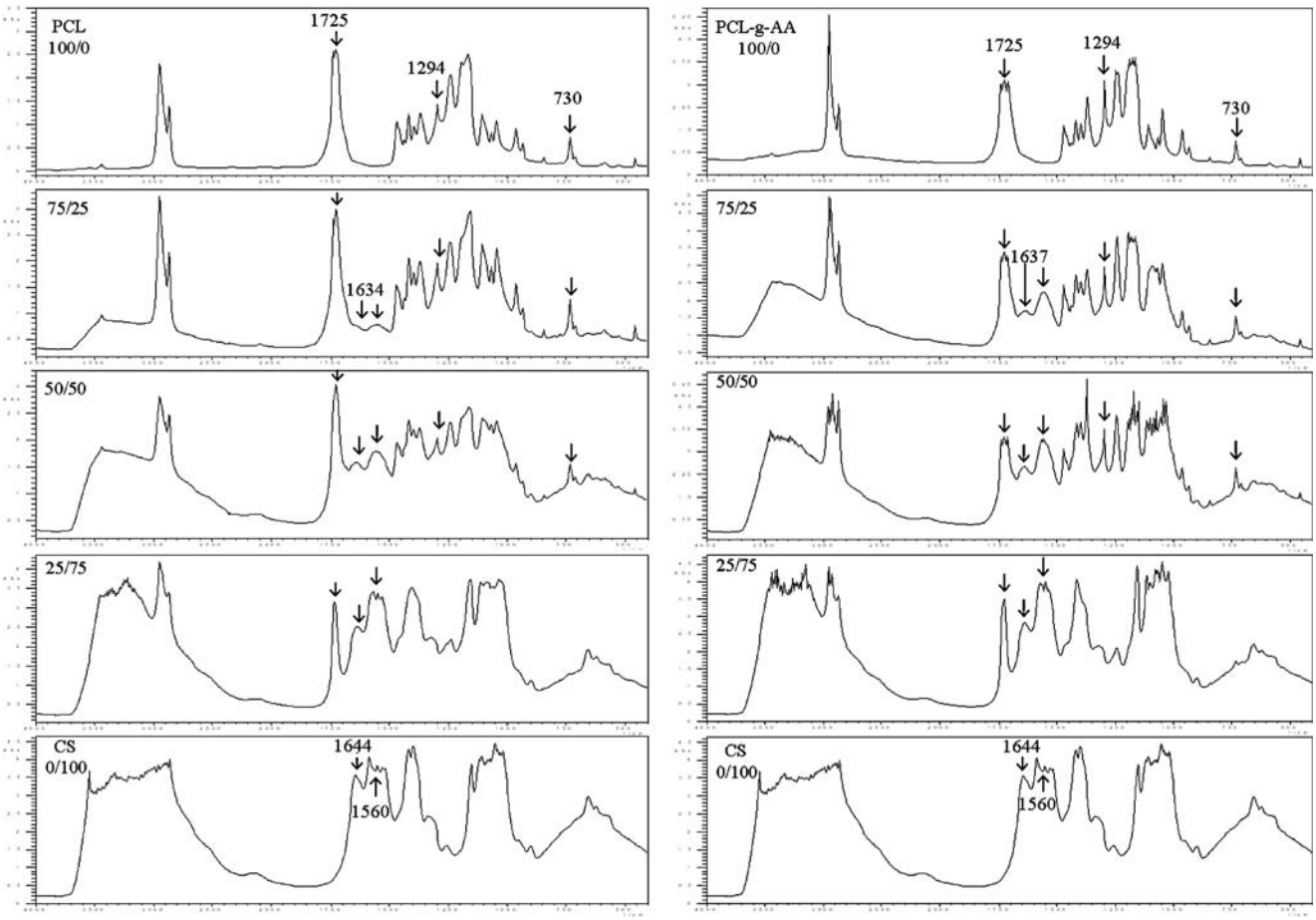


(a) PCL/CS blends (b) PCLgAA/CS blends

**Fig. 2** FTIR spectra of PCL, PCLgAA, CS and their blends with different compositions. (**a**) PCL, CS, and PCL/CS blends; (**b**) PCLgAA, CS and PCLgAA/CS blends

stretch of C=O in the amide group), and around 1560 $cm^{-1}$ (stretch of C-N and bend of N-H in the amide), also weakened with decreasing CS content. Moreover, the amino band of CS component at 1644 $cm^{-1}$ was slightly shifted to a lower frequency as the CS content decreased. When CS content was at 25 wt%, the wavenumber of the amino band decreased about 10 $cm^{-1}$ relative to that of pure CS. From this result it can be said that the intermolecular hydrogen bonds were mainly formed between the carbonyl groups of PCL and the amide groups of CS. However, it is difficult to elucidate from the FTIR spectra alone that other hydrogen-donating groups, i.e., the hydroxyl groups of CS, would contribute to the hydrogen-bonding interaction with PCL carbonyls (12,14).

Furthermore, the peak absorbance of the two bands (at 1650 and 1580 $cm^{-1}$) of amide group in the PCL/CS blends seemed to decrease proportionally with the decrease in the CS content (Fig. 2a), and nearly vanish at 25 wt% CS. However, the decrease in the same peak intensities in the PCLgAA/CS blends appeared to be less obvious (Fig. 2b), and even at 25 wt% CS, the peak intensity was still significant relative to its PCL/CS counterpart. In short, the peak absorbance of the amide group of PCLgAA/CS blends was significantly stronger than that of PCL/CS blends at the same CS content. This result, similar to that obtained by Nge et al. [28], indicated that in the blending of PCLgAA with chitosan, part of the primary amide of CS may react with the carboxyl group of PCLgAA.

In addition, in all FTIR spectra of the blends, the band at 1294 $cm^{-1}$ was assigned to the backbone C–C and C–O stretching modes in the crystalline PCL according to Coleman and Zarian [29]. Moreover, the $CH_2$ rocking band at 726 $cm^{-1}$ may also be assigned to the crystalline-sensitive band of PCL [30]. Thus, taking into account the 45% degree of crystallinity of neat PCL, we can justify the presence of the strong bands at both 1294 and 726 $cm^{-1}$ in the IR spectrum of both blends. Both bands became weaker as CS content increases, and they nearly disappear at 75 wt % of CS. These results indicated that hydrogen bonds exist between the two components in the blends, and the crystallization of PCL and PCLgAA components was suppressed by the addition of CS. The change in the crystallinity of these blends was in accordance with above DSC results.

We then investigated the FTIR spectra of PCL and the PCL/CS blends with different compositions in carbonyl region shown in Fig. 3a. For neat PCL, its carbonyl band generally consisted of two parts: crystalline and amorphous (13,14), which were difficult to resolve. After blending with CS, the carbonyl stretching bands of PCL component became remarkably weak, and the IR absorbance obviously declined with increasing CS content. Fig. 3b presents the

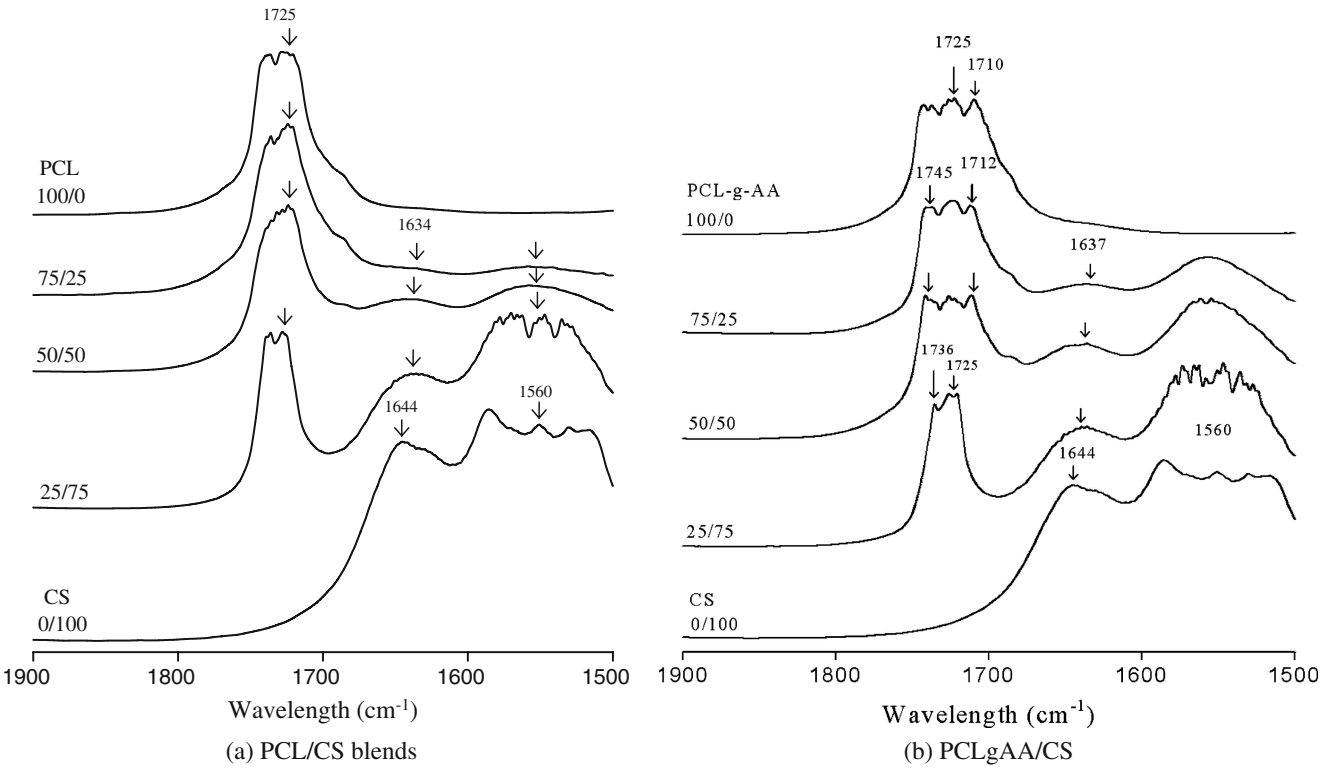


**Fig. 3** FTIR spectra of the blends in carbonyl regions. (**a**) PCL and PCL/CS blends; (**b**) PCLgAA and PCLgAA/CS blends

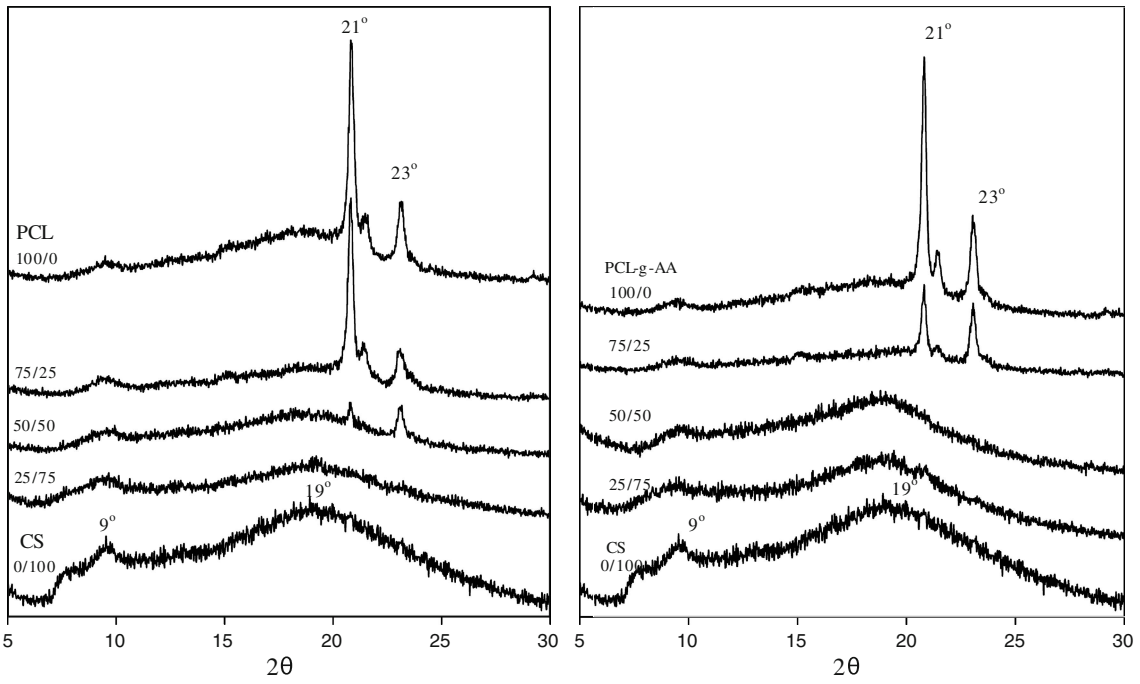


**Fig. 4** WAXD diffractograms of PCL, PCLgAA, CS and their blends with different compositions. (**a**) PCL, CS, and PCL/CS blends; (**b**) PCLgAA, CS and PCLgAA/CS blends

spectra of PCLgAA/CS blends showing additional unique absorption peaks at 1717 and 1745 $cm^{-1}$. The peak at 1717 $cm^{-1}$ was assigned to –C=O in the imide linkage (N $(COR)_2$) while the peak at 1745 $cm^{-1}$ was assigned to absorption of –C=O in the ester linkage (OCOR) (20). These new bands further justified the formation of ester and imide functional groups via the reaction between the carboxyl groups of PCLgAA and the hydroxyl and the amide groups of chitosan, when the two polymers were blended. Zong et al. [31] studied acylated chitosan copolymers with similar results.

In order to further ascertain the covalent bond formation, we also carried out the experiments to see whether the blend can be separated. The PCLgAA/CS blend membrane with 50 wt% of each component was washed with dichloromethane, a good solvent for PCLgAA, and 0.2 M aqueous acetic acid for CS, then rinsed with water, filtered, and finally dried overnight. The weight loss of PCLgAA after washing with dichloromethane was about 59 wt%, and the weight loss of CS after washing with aqueous acetic acid was about 84 wt%. In contrast, there was almost nothing left after washing the PCL/CS blends. Apparently, the residuals from PCLgAA/CS blend demonstrated the formation of covalent bonds which could not be affected by both solvents. In any case, more quantitative analysis such as NMR spectroscopy shall be pursued in the future.

## Wide-angle X-ray diffraction

The effect of intermolecular interaction on the crystallization structure of the PCL and PCLgAA/CS blends were studied using WAXD. The diffraction patterns of the blends with different compositions are shown in Fig. 4a, b. If there were no interactions between those components, the diffraction peaks should remain sharp and well defined. However, as shown in both figures, the reflection of CS at 9° disappeared in nearly all the blends, and the strong reflection at 19° was only observed in the spectrum of the blend with 75 wt% CS owing to high CS content. This indicated that the crystallization of CS molecules was almost impeded after blending with PCL or PCLgAA due to intermolecular interactions between these components, as also seen in FTIR analysis.

The diffraction peaks at 21 and 23° were ascribed to the PCL crystals [13–15]. As CS content in the blends increased, both reflections of PCL and PCLgAA components became weaker, implying that the crystallinity of PCL and PCLgAA components in the blends declined, which was also supported by above DSC and IR results. However, PCLgAA/CS blends showed a difference to the PCL/CS blends. As shown in Fig. 4b, the areas of the diffraction centered at 21 and 23° decreased drastically when a small amount of CS is blended with PCLgAA. It seemed that a small amount of CS will greatly suppressd the crystalliza-

tion of PCLgAA. Although both PCL and PCLgAA molecules can form intermolecular hydrogen bonds with CS molecules, CS molecules have the capacity to form covalent bonds with the PCLgAA molecules [20,31]. As a result, CS showed greater miscibility with PCLgAA than with PCL. When CS blends with PCLgAA, the CS molecules dispersed very well into the PCLgAA matrix and form both intermolecular hydrogen bonds and covalent bonds with the PCLgAA molecules, resulting in the significant suppression of the PCLgAA crystallization. Further, comparing the spectrum of pure PCL and PCLgAA with those of the blends, it can be seen that the d-spacing values were constant for all crystallographic planes, which indicated that the PCL or PCLgAA unit cell was not changed after blending with CS. During the crystallization of the blends, CS segments were excluded from the crystal lattice of PCL and PCLgAA. Although the crystal structure of the blends was not changed when CS is blended, the existence of hydrogen bonds and chemical covalent bonds affected the crystallization of the blends. In a previous study on the blends of CS and PEG [3], crystallinity and intermolecular interaction played an important role in improving the mechanical properties of CS. Hence, in the present study with similar crystallization behavior and intermolecular interaction, we can predict that the ductility of CS will be improved after blending with PCL or PCLgAA.

## Mechanical tensile test

All membranes had a uniform thickness of 50–60 μm in the dry state measured with a thickness gauge, and they were tested for tensile properties at room temperature. Typical stress–strain curves obtained from the PCL/CS blends were shown in Fig. 5a, whereas those from the PCLgAA/CS blends were shown in Fig. 5b. In both figures, it clearly showed that the pure CS membrane was very brittle, exhibiting a break strain as low as 8–12%, very high tensile strength (22–30 MPa), and a tensile modulus of 1200–1400 MPa (see Table 2). On the other hand, PCL membrane cast after dissolving in glacial acetic acid have a tensile modulus of 360 MPa, a tensile strength of 13 MPa, and very high tensile strain of 420–480% (see Table 2). The high ductility is the targeted property for the blends, and in blending with CS would provide materials with wide range of tensile properties. For pure PCLgAA membrane, both tensile modulus and elongation at break are only slightly lower than that of PCL. But the elongation at break is much smaller in PCLgAA membrane. It may be caused by the inhomogeneous dispersion of PCLgAA in glacial acetic acid, as will be seen from the morphological observation in the next section.

We next investigate the tensile behaviors of the blend membranes. In Fig. 5a, b, the PCL and PCLgAA/CS blends

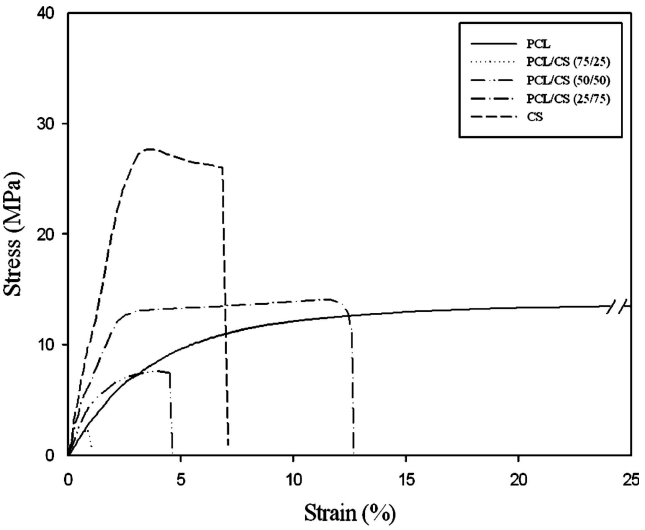


(a) PCL/CS

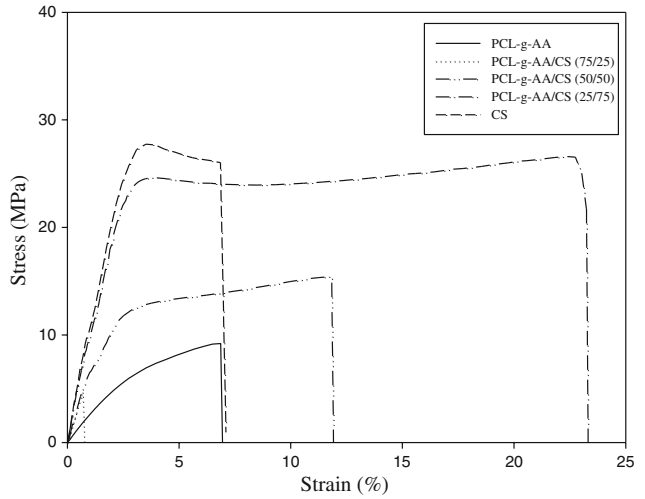


(b) PCLgAA/CS

**Fig. 5** Tensile stress-strain curves of PCL, PCLgAA, CS and their blends with different compositions. (a) PCL, CS, and PCL/CS blends; (b) PCLgAA, CS and PCLgAA/CS blends

with 75/25 composition had undergone brittle fracture at less than 1% strain. This indicated phase-separated blends because of the poor miscibility of both PCL and PCLgAA in aqueous acetic acid. In fact, the pure PCL and PCLgAA polymers can only be dissolved in aqueous acid solution at high temperatures, and they cannot form uniform membranes even drying at 55°C. On the contrary, the 25/75 blends displayed ductile behavior with a prominent yield peak before necking and cold drawing with an ultimate nominal strain above 13%. This is an indication of reinforcement, given that the individual components behaved cohesively in the blends. When comparing PCLgAA/CS blends with PCL/CS blends (see Table 2), it was obvious that the tensile properties of the former were significantly greater than that of the latter except at 25 wt%

**Table 2** Tensile properties of PCL, PCLgAA, CS and their blends

| Sample composition | Tensile Modulus(MPa) | | Tensile Strength (MPa) | | Strain at break (%) | |
|---|---|---|---|---|---|---|
| | PCL | PCL-g-AA | PCL | PCL-g-AA | PCL | PCL-g-AA |
| 100/0 | 358.9±36 | 284.0±12 | 13.0±0.46 | 10.5±2.2 | 453.0±29 | 7.0±2.3 |
| 75/25 | 403.1±74 | 802.8±109 | 3.3±0.95 | 4.5±1.2 | 0.97±0.08 | 0.61±0.098 |
| 50/50 | 559.5±11 | 911.0±55 | 7.9±1.90 | 16.3±1.7 | 5.27±1.3 | 11.8±1.8 |
| 25/75 | 940.9±76 | 1235±179 | 14.6±2.1 | 26.2±0.67 | 13.1±1.05 | 22.6±0.98 |
| CS | 1392±120 | | 26.0±4.87 | | 9.75±2.48 | |

of CS. The grafted carboxylic groups certainly enhanced the affinity between PCLgAA and CS through the covalent bond formation as seen in FTIR results. The degree of phase separation also significantly reduced in PCLgAA/CS blends as will be revealed in SEM micrographs. The above results confirmed the synergism in tensile properties of PCLgAA/CS blends, which was an indication that PCLgAA was an effective modifier for brittle CS. It could therefore be inferred that the contrast in tensile properties resulted from the differences in the internal structures of the blends, which were consequences of the enhanced intermolecular interactions between PCLgAA and CS.

## Enzymatic degradation and morphological characterization

Since the blend membranes with 25 wt% CS exhibited poor tensile properties, we only consider the enzymatic degradation of membranes with higher CS content. The results of the enzymatic degradation of the neat PCL, PCLgAA, and their CS blends in the presence of lysozyme are shown in Fig. 6. As can be seen from the weight loss curve of pure CS, the degradation of CS was not very fast, which was comparable to the 25/75 blend of PCL/CS, despite a very high concentration of lysozyme relative to physiological levels. This was attributed to the 85% DD chitosan used in this study as previous research has shown that highly deacetylated chitosan was less susceptible to the attack of lysozyme [32]. On the other hand, the weight of the neat PCL and PCLgAA appeared nearly unchanged throughout the test, indicating only the CS, which is a polysaccharide, would be subjected to the attack of lysozyme. Note that the weight of PCLgAA membrane seemed to increase slightly more than the initial weight due to the high water intake in the PCLgAA membrane (20).

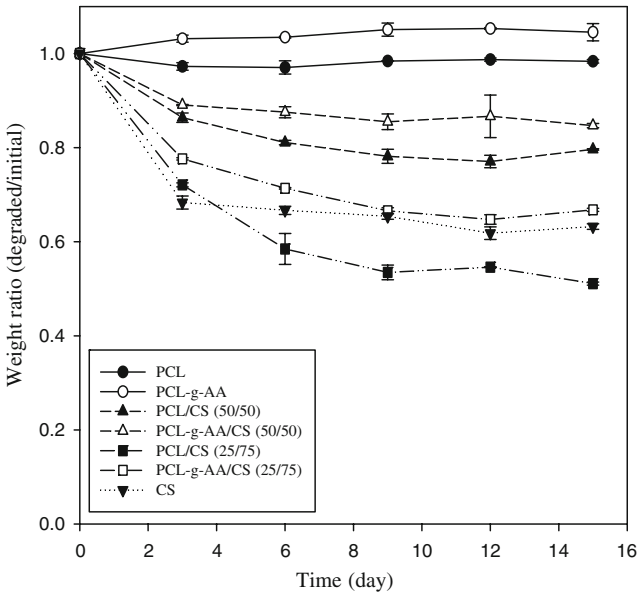


**Fig. 6** Enzymatic degradation of PCL, PCLgAA, CS and their blends with different compositions

The slopes of the weight loss-time curves can be viewed as the enzymatic degradation rates. Therefore, the neat PCL and PCLgAA samples showed the vanishing degradation rate, since it was much easier for lysozyme to degrade a polysaccharide chain of CS consisting of N-acetyl glucosamine in the blend [33], while PCL is an aliphatic polyester. Moreover, the degradation rates of the homogeneous blend membranes were increasing with increasing CS content as seen in Fig. 6. However, the degradation of the CS blends also nearly stopped after ca. 10 days, which further demonstrated that the lysozyme-mediated degradation would degrade only the CS component. Note that the weight loss of the PCL/CS blends was also greater than the PCLgAA/CS blends.

The surface morphologies of the neat samples and the blends before and after enzymatic degradation were shown in Figs. 7 and 8. Figure 7a, b showed the surface morphologies of the neat PCL before and after degradation, respectively; and similarly, Fig. 7c, d were the images of the neat PCLgAA before and after degradation. Both samples did not exhibit any change after incubated in the PBS solution of lysozyme for 12 days. Note that there were some obvious defects between spherulites on the surface of the PCLgAA membrane in Fig. 7c due to irregular arrangement of grafted acrylic acid, which would be the major cause for the low tensile strain of neat PCLgAA. Moreover, while the surface was featureless for the neat CS membrane before degradation (see Fig. 7e), there was obvious surface erosion after degradation in Fig. 7f, where

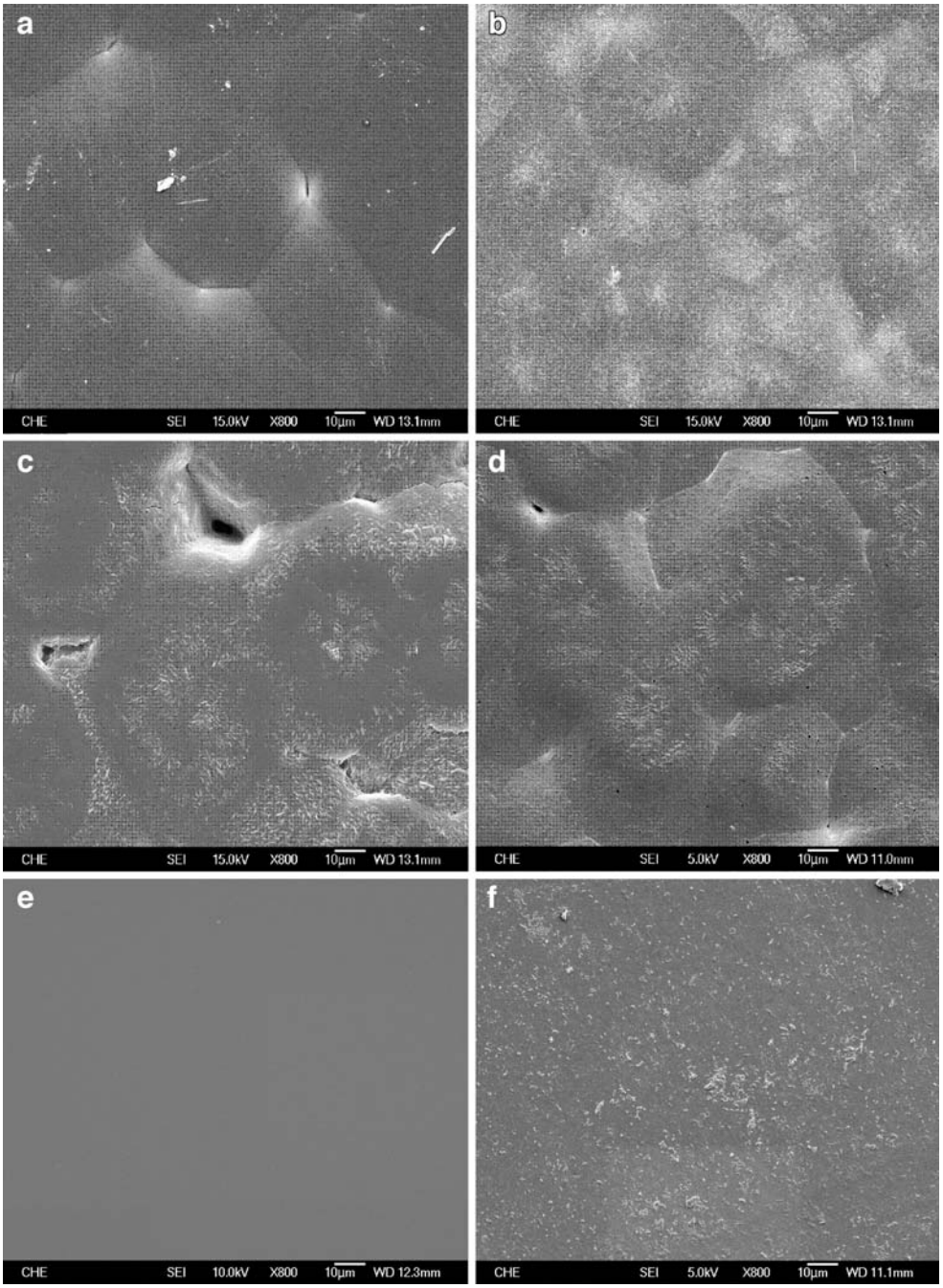


**Fig. 7** SEM micrographs of neat polymer membranes. (**a**) PCL before degradation; (**b**) PCL after degradation for 12 d; (**c**) PCLgAA before degradation; (**d**) PCLgAA after degradation for 12 d; (**e**) CS before degradation; (f) CS after degradation for 12 d

the membrane surface was littered with small chips of CS residuals.

Next, Fig. 8a, b showed the surface morphologies of 25/75 PCL/CS blend before and after degradation, respectively. While the surface of the blend membrane before degradation was seemingly smooth, there were some nearly spherical droplets embedded in the CS matrix (see Fig. 8a). After degradation, the homogeneous erosion of the blend surface was clearly seen (see Fig. 8b). Since only the CS molecules were eroded, the PCL molecules emerged as spherical droplets on the membrane surface, suggesting that PCL and CS were only partially miscible and the blends are phase-separated. Figure 8c, d showed the surface morphologies of 25/75 PCLgAA/CS blend before and after degradation, respectively. It can be seen that the surface morphology of PCLgAA/CS blend (see Fig. 8c) was more homogeneous than that of the PC/CS blend, which confirmed the improved miscibility between PCLgAA and CS. After the degradation of CS component at the surface of the blend membrane, the PCLgAA molecules also appeared as spherical droplets on the membrane surface (see Fig. 8d), and the droplet size appeared more uniform than the PCL droplet. It may be concluded that PCLgAA was dispersed more uniformly in the CS matrix. Further-

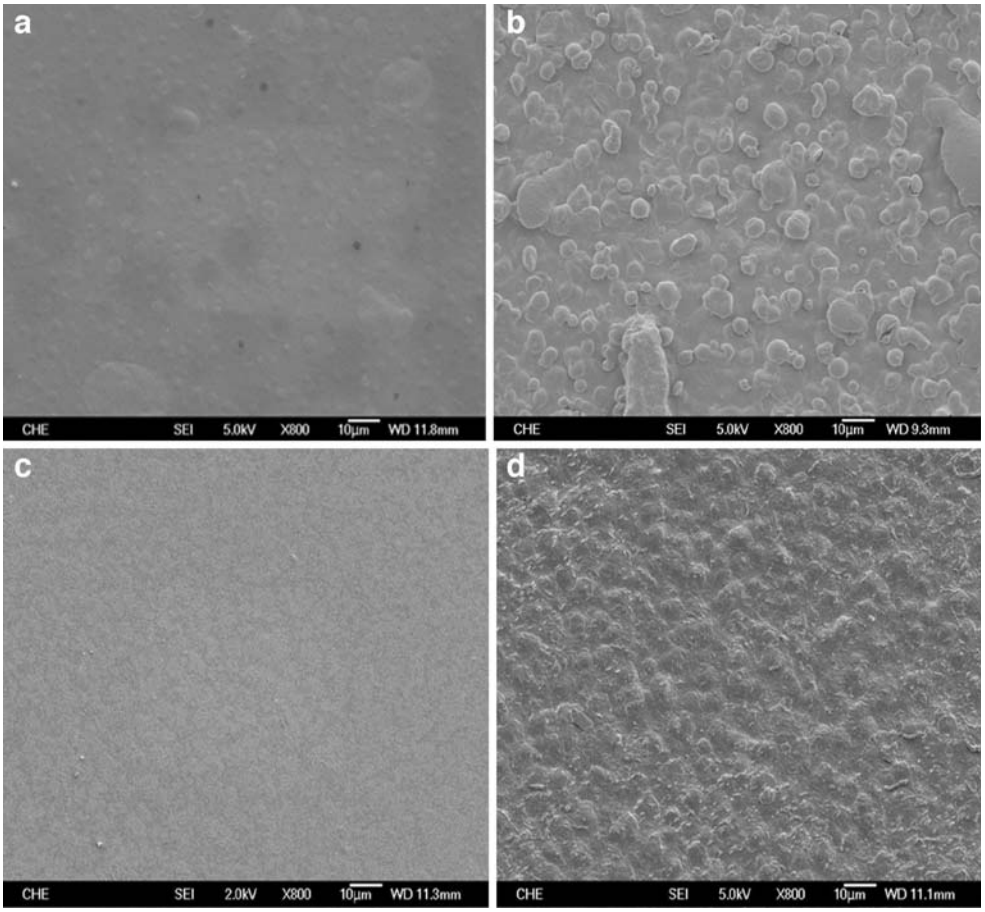


**Fig. 8** SEM micrographs of blend membranes with composition at 25/75

more, when comparing Fig 8b, d, it is apparent that the extent of the surface erosion of the PCL/CS blend was far greater than that of the PCLgAA/CS blend. We then may want to know why the PCL/CS and PCLgAA/CS samples showed different enzymatic degradation rates. Note that chitosan is a crystallizable polymer, and the addition of PCL or PCLgAA aspparently influenced the crystallization of CS in these blends as seen from the WAXD results. Even though the suppression of the CS crystallization in the PCLgAA/CS blends was found to be more severe than in the PCL/CS blends, the resistance to the biodegradation of PCLgAA/CS membranes was more pronounced due to the enhanced affinity through covalent bond formation mainly in the amorphous phase between PCLgAA and CS molecules.

## Conclusions

In this work, PCL and PCLgAA/CS biodegradable polyester/polysaccharide blends were prepared by the solvent casting method in a homogeneous solution of aqueous acetic acid. However, morphological observation with FESEM revealed a phase-separated structure of the blend membranes. The spherical droplets of the PCL and PCLgAA components were clearly seen on the membrane surfaces after lysozyme-mediated biodegradation. The extent of crystallization of these components in the blends was investigated by DSC, FTIR and WAXD spectroscopy. The degree of crystallinity of PCL and PCLgAA, determined by DSC, decreased upon blending with CS. This result was confirmed by FTIR spectroscopy. FTIR spectra showed that the PCL carbonyls formed intermolecular hydrogen bonds with CS. However, the PCLgAA molecules have the capacity to form covalent bonds with the CS molecules through the grafted carboxlic acid in PCLgAA, which suppressed the crystallization of CS more severely. In addition, the resulting crystalline structure of the PCL and PCLgAA components was not affected as seen in WAXD diffractogram. Analysis of tensile properties of the blend membranes showed the possibility of altering the mechanical properties of CS. In particular, blends with 50 and 75 wt% CS were superior to individual polymers. Overall, 25/75 ratio blend membranes of PCLgAA/CS composites showed improved tensile behaviors with the greatest ductility of all samples. Finally, it was found that the degradation rates of PCLgAA/CS membranes were lower than that of the PCL/CS ones, whereas the degradation rate of PCL/CS membrane with 75 wt% CS was close to that of the neat CS. The strong intermolecular

interaction between PCLgAA and CS in the amorphous phase slows down the enzymatic degradation despite the significant suppression of the CS crystallization in the blends. Furthermore, the cellular activity of the formed blends will be investigated in the future to explore the significant potential of the blend membranes for various tissue engineering applications.

## References


1. Shahidi F, Arachchi JKV, Jeon YJ (1999) Trends Food Sci Technol 10:37–51. doi:10.1016/S0924-2244(99)00017-5
2. Rao SB, Sharma CP (1997) J Biomed Mater Res 34:21–28. doi:10.1002/(SICI)1097-4636(199701)34:1<21::AID-JBM4>3.0.CO;2-P
3. Muzzarelli RAA, Jeuniaux C (1986) Gooday GW Chitin in nature and technology. Plenum, New York
4. Madihally SV, Matthew HWT (1999) Biomaterials 20:1133–1142. doi:10.1016/S0142-9612(99)00011-3
5. Kolhe P, Kannan RM (2003) Biomacromolecules 4:173–180. doi:10.1021/bm025689+
6. Nho YC, Park KR (2002) J Appl Polym Sci 85:1787–1794. doi:10.1002/app.10812
7. Don TM, Hsu SC, Chiu WY (2001) J Polym Sci Part Polym Chem 39:1646–1655. doi:10.1002/pola.1142
8. Ha BJ, Lee YS (1998) Adv Chitin Sci 3:160–164
9. Piekielna J, Mucha M, Szwarc M (1997) Adv Chitin Sci 2:537–542
10. Mucha M, Piekielna J, Wieczorek A (1999) Macromol Symp 144:391–412
11. Alexeev VL, Kelberg EA, Evmenenko GA (2000) Polym. Eng Sci 40:1211–1215. doi:10.1002/pen.11248
12. Chen C, Dong L, Cheung MK (2005) Eur Polym J 41:958–966. doi:10.1016/j.eurpolymj.2004.12.002
13. Senda T, He Y, Inou Y (2001) Polym Int 51:33–39. doi:10.1002/pi.793
14. Honma T, Senda T, Inoue Y (2003) Polym Int 52:1839–1849. doi:10.1002/pi.1380
15. Honma T, Zhao L, Asakawa N, Inoue Y (2006) Macro Bio 6:241–249. doi:10.1002/mabi.200500216
16. Olabarrieta I, Forsstrom D, Gedde UW, Hedenqvist MS (2001) Polymer (Guildf) 42:4401. doi:10.1016/S0032-3861(00)00680-7
17. Sarasam A, Madihally SV (2005) Biomaterials 26:5500–5508. doi:10.1016/j.biomaterials.2005.01.071
18. Jang BC, Huh SY, Jang JG, Bae YC (2001) J Appl Polym Sci 82:3313–3320. doi:10.1002/app. 2190
19. Avella M, Errico ME, Laurienzo P, Martuscelli E, Raimo M, Rimedio R (2000) Polymer (Guildf) 41:3875. doi:10.1016/S0032-3861(99)00663-1
20. Wu CS (2005) Polymer (Guildf) 46:147–155. doi:10.1016/j.polymer.2004.11.013
21. Gaylord NG, Mehta R, Kumar V, Tazi M (1989) J Appl Polym Sci 38:359–371. doi:10.1002/app.1989.070380217
22. Sakurai K, Maegawa T, Takahashi T (2000) Polymer (Guildf) 41:7051–7056. doi:10.1016/S0032-3861(00)00067-7
23. Elzein T, Nasser-Eddine M, Delaite C, Bistac S, Dumas PJ (2004) Collo. Interface Sci 273:381–387. doi:10.1016/j.jcis.2004.02.001
24. Wu CS, Lai SM, Liao HT (2002) J Appl Polym Sci 85:2905–2912. doi:10.1002/app.10806
25. Kim J, Tirrell DA (1999) Macromol 32:945–948. doi:10.1021/ma981186d
26. Person FG, Marchessault RH, Liang CY (1960) J Polym Sci 43:101–107. doi:10.1002/pol.1960.1204314109
27. Cho K, Lee J, Xing P (2002) J Appl Polym Sci 83:868–879. doi:10.1002/app.10084
28. Nge TT, Yamaguchi M, Hori N, Takemura A, Ono H (2002) J Appl Polym Sci 83:1025–1035. doi:10.1002/app.10010
29. Coleman MM, Zarian J (1979) J Polym Sci [B] 17:837–850
30. Chandra R, Rustgi R (1997) Polym Degrad Stabil 56:185–202. doi:10.1016/S0141-3910(96)00212-1
31. Zong Z, Kimura Y, Takahashi M, Yamane H (2000) Polymer (Guildf) 41:899–906. doi:10.1016/S0032-3861(99)00270-0
32. VandeVord PJ, Matthew HW, DeSilva SP, Mayton L, Wu B, Wooley PH (2002) J Biomed Mater Res 59:585–590. doi:10.1002/jbm.1270
33. Phillips DC (1966) Sci Am 215:78–90